

# Potential energy surfaces for electron dynamics modeled by floating and breathing Gaussian wave packets with valence-bond spin-coupling: An analysis of high-harmonic generation spectrum

Koji Ando\*

*Department of Information and Sciences, Tokyo Woman's Christian University,  
2-6-1 Zenpukuji, Suginami-ku, Tokyo 167-8585, Japan*

(Dated: May 29, 2022)

A model of localized electron wave packets (EWPs), floating and breathing Gaussians with non-orthogonal valence-bond spin-coupling, is applied to compute the high-harmonic generation (HHG) spectrum from a LiH molecule induced by an intense laser pulse. The characteristic features of the spectrum, a plateau up to 50 harmonic-order and a cut-off, agreed well with those from the previous time-dependent complete active-space self-consistent-field calculation [T. Sato and K. L. Ishikawa, *Phys. Rev. A* **91**, 023417 (2015)]. In contrast with the conventional molecular orbital picture in which the Li 2s and H 1s atomic orbitals are strongly mixed, the present calculation indicates that an incoherent sum of responses of single electrons reproduces the HHG spectrum, in which the contribution from H 1s electron dominates the plateau and cut-off, whereas the Li 2s electron contributes to the lower frequency response. The results are comprehensive in terms of the shapes of single-electron potential energy curves constructed from the localized EWP model.

## INTRODUCTION

Electron dynamics in molecules is an emerging field of research driven by recent advances of attosecond time-resolved laser spectroscopies [1–4]. In particular, the high-harmonic generation (HHG) spectra induced by intense laser field has been a major subject [5–9] vitalized by a proposed possibility of self-probing molecules by their own electrons, which aims as far as to probe electronic wave functions (more precisely the Dyson orbitals) via the so-called molecular orbital (MO) tomography [10–13].

Theoretical studies of HHG spectra with quantum dynamical calculations of realistic systems have been rather limited to small atoms and molecules such as H, He,  $H_2^+$ ,  $H_2$ ,  $HeH^+$ ,  $D_3^+$ , and LiH [14–20]. Treating more electrons in larger and more complex molecules seems too demanding at present unless invoking the time-dependent mean-field approximations of various levels [21–27] or the density functional theory (DFT) [28–30]. The conventional MO and DFT calculations are based on atomic orbitals (AOs) that are clamped at nuclear centers, with the time-dependence carried by the coefficients of MO or the configuration-interaction. They essentially rely on the concept of one-electron orbitals in the mean-field that are normally delocalized over the molecule according to its spatial symmetry. To describe the dynamics of delocalized wave functions by spatially fixed basis functions, those of large wave numbers or high angular momenta are needed.

To obtain an alternative perspective, we have been studying a model of localized electron wave packets (EWPs) with non-orthogonal valence-bond (VB) spin-coupling [31–34]. It was originally developed for a polarizable and reactive force-field model in condensed phase simulations to be combined with nuclear wave packets for light atoms [35–38]. For small molecules such as  $H_2$ , LiH,  $BeH_2$ ,  $CH_2$ ,  $H_2O$ , and  $NH_3$  in

the ground electronic state, the model gives reasonably accurate potential energy surfaces with the minimal number of EWPs [32]. The accuracy is considered to come from the flexibility to describe the static correlation by the VB coupling, the dynamic correlation by the EWP breathing, and the polarization by the EWP floating. The electronic excited states of LiH have been also examined by quantizing the potential energy curves constructed in the same way as in this work [33]. The present work is an extension to study the real-time quantum electron dynamics. Along this line, we have reported recently the semiquantal WP dynamics of Li 2s EWP in LiH induced by an intense laser pulse [34]. The computed HHG spectrum exhibited the intensity up to a hundred of harmonic order, but not the characteristic plateau and cut-off. We considered this would be due to the lack of quantum coherence in the simple semiquantal dynamics of the localized EWP, and could be remedied by introducing the Monte Carlo integration of coherent-state path-integral (CSPI) propagator [39, 40]. Nonetheless, for a small diatomic molecule such as LiH, the full quantum dynamics in one-dimension is straightforward on the effective one-electron potential energy curves constructed from the EWPs. This will be a test for the adequacy of the model before proceeding to the CSPI calculations.

After an outline of the theory and computation in Sec. II, potential energy curves for electron motion in a LiH molecule are presented. Single-electron quantum dynamics on these potential curves induced by an intense laser pulse are computed and the HHG spectra are examined. Section IV concludes.

## THEORY AND COMPUTATION

As in our previous reports [31–34], The electronic wave function is assumed to be an antisymmetrized product of spatial and spin functions,

$$\Psi(1, \dots, N) = \mathcal{A}[\Phi(\mathbf{r}_1, \dots, \mathbf{r}_N)\Theta(1, \dots, N)], \quad (1)$$

\*E-mail: ando.k@lab.twcu.ac.jp

with the spatial part modeled by a product of one-electron functions,

$$\Phi(\mathbf{r}_1, \dots, \mathbf{r}_N) = \phi_1(\mathbf{r}_1) \cdots \phi_N(\mathbf{r}_N). \quad (2)$$

In contrast with the conventional VB methods that use the AOs clumped at nuclear centers, we employ ‘floating and breathing’ spherical Gaussian WPs of variable position  $\mathbf{q}_i$  and width  $\rho_i$ ,

$$\phi_i(\mathbf{r}) = (2\pi\rho_i^2)^{-\frac{3}{4}} \exp[-|\mathbf{r} - \mathbf{q}_i|^2/4\rho_i^2]. \quad (3)$$

In our previous report [34],  $\mathbf{q}_i$  and  $\rho_i$  were time-dependent, but in this work, the EWPs are used just to construct the effective potential energy curves along displacements of  $\mathbf{q}_i$  on which the full quantum dynamics are evolved. The spin part  $\Theta(1, \dots, N)$  consists of the spin eigenfunctions. In this work, we employ a single configuration of the perfect-pairing form,

$$\Theta = \theta(1, 2)\theta(3, 4) \cdots \theta(N-1, N), \quad (4)$$

with  $\theta(i, j) = (\alpha(i)\beta(j) - \beta(i)\alpha(j))/\sqrt{2}$ . The electronic energy,  $E = \langle \Psi | \hat{H} | \Psi \rangle / \langle \Psi | \Psi \rangle$ , is thus a function of the variables  $\{\mathbf{q}_i\}$  and  $\{\rho_i\}$  at a given nuclear geometry  $\{\mathbf{R}_I\}$ . We first optimized  $\{\mathbf{q}_i\}$  and  $\{\rho_i\}$  to minimize the energy  $E(\{\mathbf{q}_i\}, \{\rho_i\}; \{\mathbf{R}_I\})$ , to determine the optimal values  $\{\mathbf{q}_i^{(0)}\}$  and  $\{\rho_i^{(0)}\}$ . The effective potential function for the  $j$ -th electron  $\mathcal{V}_j(\mathbf{q})$  was then constructed by fixing all the variables other than  $\mathbf{q}_j$  at the optimal values,

$$\mathcal{V}_j(\mathbf{q}) = E(\mathbf{q}_1^{(0)}, \dots, \mathbf{q}_{j-1}^{(0)}, \mathbf{q}, \mathbf{q}_{j+1}^{(0)}, \dots, \mathbf{q}_N^{(0)}, \rho_1^{(0)}, \dots, \rho_N^{(0)}; \{\mathbf{R}_I\}), \quad (5)$$

on which the time-dependent Schrödinger equation was numerically solved with the effective one-electron Hamiltonian for the  $j$ -th electron,

$$\hat{\mathcal{H}}_j = -\frac{\hbar^2}{2m} \nabla_{\mathbf{q}} + \mathcal{V}_j(\mathbf{q}). \quad (6)$$

It might appear that the electronic kinetic energies were double-counted since they have been computed in  $E = \langle \Psi | \hat{H} | \Psi \rangle / \langle \Psi | \Psi \rangle$ . However, those in  $\mathcal{V}_j(\mathbf{q})$  are constants with the fixed  $\{\rho_i^{(0)}\}$  as the kinetic energy expectation for  $\phi_i(\mathbf{r})$  of Eq. (3) is  $\hbar^2/(8m\rho_i^2)$ .

Although the procedure is essentially a one-electron approximation under the field of other EWPs, it is distinct from those of MO and Kohn-Sham models. The use of such EWP potentials is related to the coherent-state path-integral theory in which the Gaussian WPs are identified as the coordinate representation of the coherent-state basis and the action integral is determined by the energy expectation with respect to the WPs [39, 40]. It also has a technical advantage of removing the singularity of Coulomb potential that can cause problems with the numerical grid methods of quantum dynamical calculation. (This problem would be a reason for the use of soft Coulomb potential of a form  $1/\sqrt{r^2 + c}$  in many of the

previous studies, including Ref. [27] with which our results will be compared.)

The scheme was applied to a LiH molecule under an intense laser pulse. The parameters were taken from Ref. [27] that employed the time-dependent complete-active-space self-consistent-field (TD-CASSCF) calculation. The internuclear distance was fixed at 2.3 bohr. The EWP centers  $\mathbf{q}_j$  were displaced along the bond direction and the electronic energies were calculated to construct the potential curves  $\mathcal{V}_j(\mathbf{q})$  in one-dimension. The electron dynamics were induced by a laser pulse with time-dependent electric field

$$\mathcal{E}(t) = \mathcal{E}_0 \sin(\omega_0 t) \sin^2(\pi t/\tau), \quad 0 \leq t \leq \tau, \quad (7)$$

parallel to the bond direction. The frequency  $\omega_0$  corresponds to the wavelength of 750 nm, the duration  $\tau$  is of three optical cycles,  $\tau = 3(2\pi/\omega_0) \simeq 7.51$  fs, and the field intensity  $\mathcal{E}_0$  is  $5.5 \times 10^8$  V/cm with the laser intensity  $4.0 \times 10^{14}$  W/cm<sup>2</sup>. The length of the simulation box was taken to be 1200 bohr, with the transmission-free absorbing potential [41] of 120 bohr length at both ends. The initial condition of the electronic wave function at  $t = 0$  was a Gaussian function of the center  $\mathbf{q}_j^{(0)}$  and width  $\rho_j^{(0)}$ , i.e., those optimized without the external field. The wave functions were propagated with the Cayley’s hybrid scheme [42] with the spatial grid length of 0.2 bohr and the time-step of 0.01 au ( $\sim 0.24$  as). The norm of the wave function stayed unity with the deviation less than  $10^{-7}$  throughout the simulation. The HHG spectra were computed from the Fourier transform of the dipole acceleration dynamics.

We note that the quantum dynamical calculations in this work are one-dimensional: the EWPs are spherical in three-dimension, but they are used just to construct the effective potential curves  $\mathcal{V}_j(\mathbf{q})$  along the bond axis. The one-dimensional treatment is in accord with the TD-CASSCF calculation of Ref. [27] which we take as the reference for comparison.

## RESULTS AND DISCUSSION

Figure 1 displays the potential energy curves  $\mathcal{V}_j(\mathbf{q})$  for the electrons in LiH. Two of them are deeply bound to the Li nuclear center and correspond to the Li 1s core electrons. Their contributions to the HHG spectrum have been analyzed previously with the ordinary frozen-core treatment [27]. Therefore, we focus on the more labile Li 2s and H 1s electrons with much shallower potential wells in Fig. 1. The potentials for EWPs are modulated under the external laser field via the field-dipole interaction. The modulations at the maximum and minimum of the field  $\mathcal{E}(t)$  in Eq. (7) (see also the upper panel of Fig. 3) are displayed in Fig. 2. The potentials indicate that the dynamics of Li 2s electron will be directly driven by the laser field without energy barriers, whereas the H 1s electron will be basically bound near the proton but with possibilities of tunneling out in both directions. These pictures are confirmed in Fig. 3 that plots the position expectation and

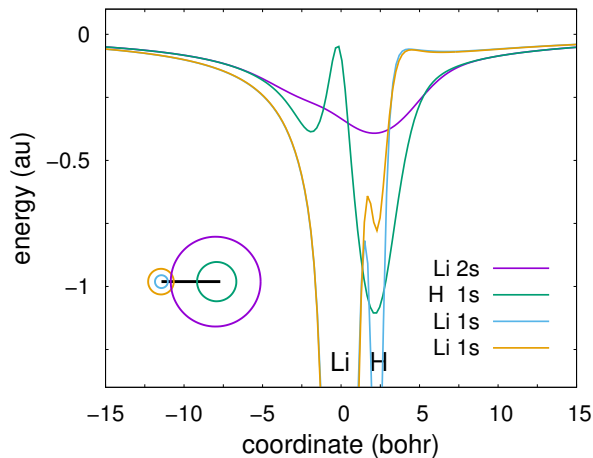


FIG. 1: Potential energy curves for displacements of the wave packet centers in the singlet  $X^1\Sigma^+$  state of LiH. The inset shows the wave packets represented by circles with the radius of wave packet width  $\rho_i$

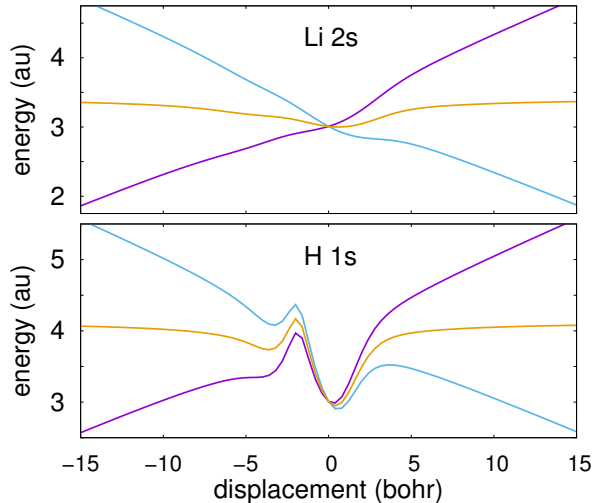


FIG. 2: Potential energy curves for Li 2s and H 1s electron wave packet centers modulated by the laser field of Eq. (7) via the field-dipole interaction.

its root-mean-squares (rms) deviation of the time-dependent wave function.

Figure 4 displays the HHG spectra from the dipole acceleration dynamics of Li 2s and H 1s electrons, and their incoherent sum with an equal weight, as the dipole moment is additive, neglecting the cross-correlation in the power spectrum. For comparison, data from the TD-CASSCF calculation [27] was included. It is seen that the incoherent sum of the Li 2s and H 1s spectra agrees well with the TD-CASSCF spectrum, particularly the plateau up to  $\sim 50$  harmonic order (HO) and the cut-off. The spectra from individual electrons indicate that the plateau and cut-off come almost solely from the H 1s dynamics. The spectrum of Li 2s electron dominates

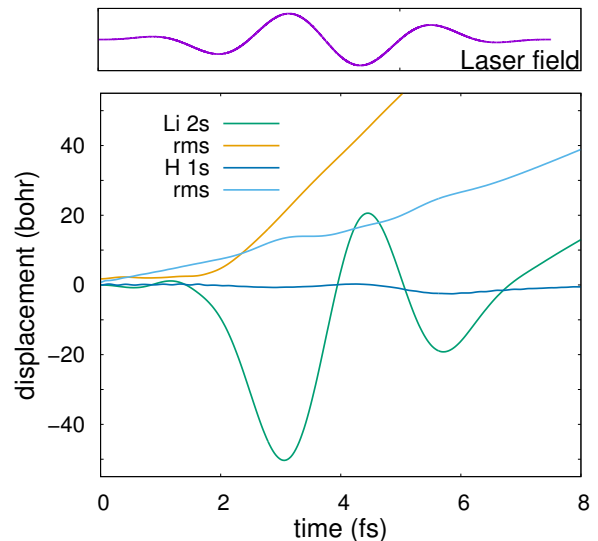


FIG. 3: Time evolution of the position expectation value and its root-mean-squares (rms) deviation. The upper panel displays the laser field of Eq. (7).

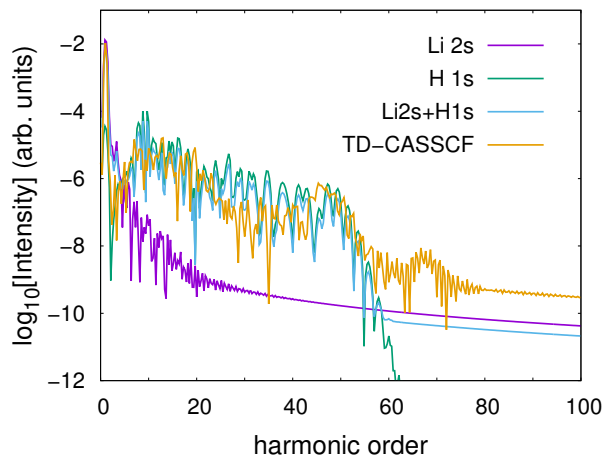


FIG. 4: Fourier transforms of the dipole acceleration that give the high-harmonic generation spectra. The abscissa is the harmonic order  $\omega/\omega_0$ . The TD-CASSCF data is from Ref. [27].

the low-frequency peak at 1 HO, but decays by  $\sim 20$  HO. This is comprehended in terms of the potential shape and its modulation in the upper panel of Fig. 2: the potential well for Li 2s EWP is shallow such that the dynamics will be rather similar to that of a free electron directly driven by the external field, which will result in the dominant contribution of the first HO in the spectrum. The agreement of the incoherent sum with the TD-CASSCF spectrum also implies that the correlation between the H 1s and Li 2s electrons is minor. This is again comprehensive with the results in Fig. 3: the small amplitude oscillation of the position expectation of H 1s electron indicates that the mean-field treatment for the calculation of Li 2s electronic potential was adequate, and the dynamics of these

two electrons with different amplitudes of spatial oscillation are mostly decoupled.

In the conventional MO picture, the Li 2s and H 1s AOs are strongly mixed in the valence MOs, from which the time-dependent wave functions are described by mixing many configuration state functions. The picture is thus fundamentally different from the present VB WP, but by applying some localization or projection analysis to the complex MO-CI wave function, a connection might be found. Similar argument would apply to the picture of population transfers among MOs, in particular, the natural orbitals [24, 26, 43]: in this case, a projection of the present wave functions to the conventional natural orbitals would complement the picture. Another intriguing issue is on the different treatments of Coulomb interaction, the soft Coulomb potential in Ref. [27] and the ordinary Coulomb potential in the present work. The present scheme removes the singularity of  $1/r$  by averaging with the EWPs  $\phi_i(\mathbf{r})$ , to give an effectively softened potential  $\mathcal{V}_j(\mathbf{q})$  without empirical adjustments.

## CONCLUSION

The single-electron quantum dynamics on the electronic potential energy curves constructed with use of the localized floating and breathing electron wave packets with the VB spin-coupling produced the HHG spectrum of a LiH molecule in good agreement with the previous TD-CASSCF calculation. The electronic potential energy curves provides a unique picture for understanding the dynamics. Although more case studies and improvements for numerical efficiencies are needed, we envisage that its applications will extend not only to other molecules but also to the electron conduction and optical processes in condensed matters.

## Acknowledgment

This work was supported by KAKENHI No. 26248009 and 26620007. The author is grateful to Professors Takeshi Sato and Kenichi Ishikawa for providing their data in Ref. [27].

---

[1] P. H. Bucksbaum, *Science* **317**, 766 (2007).  
 [2] M. F. Kling and M. J. J. Vrakking, *Ann. Rev. Phys. Chem.* **59**, 463 (2008).  
 [3] F. Krausz and M. Ivanov, *Rev. Mod. Phys.* **81**, 163 (2009).  
 [4] K. Ramasesha, S. R. Leone, and D. M. Neumark, *Ann. Rev. Phys. Chem.* **67**, 41 (2016).  
 [5] J. L. Krause, K. J. Schafer, and K. C. Kulander, *Phys. Rev. Lett.* **68**, 3535 (1992).  
 [6] K. J. Schafer, B. Yang, L. F. DiMauro, and K. C. Kulander, *Phys. Rev. Lett.* **70**, 1599 (1993).  
 [7] P. B. Corkum, *Phys. Rev. Lett.* **71**, 1994 (1993).  
 [8] J. C. Baggesen and L. B. Madsen, *J. Phys. B: At. Mol. Opt. Phys.* **44**, 115601 (2011).

[9] A. D. Bandrauk, F. Fillion-Gourdeau, and E. Lorin, *J. Phys. B: At. Mol. Opt. Phys.* **46**, 153001 (2013).  
 [10] J. Itatani, J. Levesque, D. Zeldler, H. Niikura, H. Pépin, J. C. Kleffer, P. B. Corkum, and D. M. Villeneuve, *Nature* **432**, 867 (2004).  
 [11] S. Haessler, J. Caillat, and P. Salières, *J. Phys. B: At. Mol. Opt. Phys.* **44**, 203001 (2011).  
 [12] P. Salières, A. Maquet, S. Haessler, J. Caillat, and R. Taïeb, *Rep. Prog. Phys.* **75**, 062401 (2012).  
 [13] H. Offenbacher, D. Lüftner, T. Ules, E. M. Reinisch, G. Koller, P. Puschnig, and M. G. Ramsey, *J. Electron. Spectrosc. Relat. Phenom* **204**, 92 (2015).  
 [14] F. Grossmann, *Theoretical Femtosecond Physics: Atoms and Molecules in Strong Laser Fields* (Springer, Heidelberg, 2013).  
 [15] D. Geppert, P. von den Hoff, and R. de Vibie-Riedle, *J. Phys. B: At. Mol. Opt. Phys.* **41**, 074006 (2008).  
 [16] N. Takemoto and A. Becker, *Phys. Rev. A* **84**, 023401 (2011).  
 [17] F. Remacle and R. D. Levine, *Phys. Rev. A* **83**, 013411 (2011).  
 [18] E. Lötstedt, T. Kato, and K. Yamanouchi, *Phys. Rev. A* **85**, 053410 (2012).  
 [19] O. I. Tolstikhin, H. J. Wörner, and T. Morishita, *Phys. Rev. A* **87**, 041401(R) (2013).  
 [20] P. C. Li, Y. L. Sheu, H. Z. Jooya, X. X. Zhou, and S. I. Chu, *Sci. Rep.* **6**, 32763 (2016).  
 [21] H. B. Schlegel, S. M. Smith, and X. Li, *J. Chem. Phys.* **126**, 244110 (2007).  
 [22] M. Nest, F. Remacle, and R. D. Levine, *New. J. Phys.* **10**, 025109 (2008).  
 [23] T. Yonehara and K. Takatsuka, *J. Chem. Phys.* **128**, 154104 (2008).  
 [24] T. Kato, T. Oyamada, H. Kono, and S. Koseki, *Prog. Theor. Phys. Suppl.* **196**, 16 (2012).  
 [25] D. J. Haxton, K. V. Lawler, and C. W. McCurdy, *Phys. Rev. A* **86**, 013406 (2012).  
 [26] S. Ohmura, H. Kono, T. Oyamada, T. Kato, K. Nakai, and S. Koseki, *J. Chem. Phys.* **141**, 114105 (2014).  
 [27] T. Sato and K. L. Ishikawa, *Phys. Rev. A* **91**, 023417 (2015).  
 [28] E. P. Fowe and A. D. Bandrauk, in *Coherence and Ultrashort Pulse Laser Emission*, ed. F. J. Duarte pp. 493–518 (2010).  
 [29] V. Kapoor, M. Ruggenthaler, and D. Bauer, *Phys. Rev. A* **87**, 042521 (2013).  
 [30] D. A. Telnov, K. E. Sosnova, E. Rozenbaum, and Shih-I. Chu, *Phys. Rev. A* **87**, 053406 (2013).  
 [31] K. Ando, *Bull. Chem. Soc. Jpn.* **82**, 975 (2009).  
 [32] K. Ando, *Chem. Phys. Lett.* **523**, 134 (2012).  
 [33] K. Ando, *J. Chem. Phys.* **144**, 124109 (2016).  
 [34] K. Ando, *Comp. Theor. Chem.* **1116**, 159 (2017).  
 [35] K. Hyeon-Deuk and K. Ando, *J. Chem. Phys.* **140**, 171101 (2014).  
 [36] K. Hyeon-Deuk and K. Ando, *Phys. Rev. B* **90**, 165132 (2014).  
 [37] K. Hyeon-Deuk and K. Ando, *J. Chem. Phys.* **144**, 171102 (2015).  
 [38] K. Hyeon-Deuk and K. Ando, *Phys. Chem. Chem. Phys.* **18**, 2314 (2016).  
 [39] H. Kuratsuji, *Prog. Theor. Phys.* **65**, 224 (1981).  
 [40] K. Ando, *Chem. Phys. Lett.* **591**, 179 (2014).  
 [41] T. Gonzalez-Lezana, E. J. Rackham, and D. E. Manolopoulos, *J. Chem. Phys.* **120**, 2247 (2004).  
 [42] N. Watanabe and M. Tsukada, *Phys. Rev. E* **62**, 2914 (2000).  
 [43] M. Brics, J. Rapp, and D. Bauer, *Phys. Rev. A* **93**, 013404 (2016).